CHEMICAL ENGINEERING TRANSACTIONS
VOL. 56, 2017
A publication of AIDIC
The Italian Association of Chemical Engineering
Online at www.aidic.it/cet
Guest Editors: Jiří Jaromír Klemeš, Peng Yen Liew, Wai Shin Ho, Jeng Shiun Lim

ISBN 978-88-95608-47-1; **ISSN** 2283-9216
DOI: 10.3303/CET1756266

The Effect of Air Gap on the Morphological Properties of PSf/PVP90 Membrane for Hemodialysis Application

Noresah Said[a], Hasrinah Hasbullah[a], Ahmad Fauzi Ismail[a], Muhammad Nidzhom Zainol Abidin[a], Pei Sean Goh[a], Mohd Hafiz Dzarfan Othman[a], Siti Hamimah Sheikh Abdul Kadir[b], Fatmawati Kamal[b], Mohd Sohaimi Abdullah[a], Be Cheer Ng[a]

[a]Advanced Membrane Technology Research Centre (AMTEC), Universiti Teknologi Malaysia, 81310 UTM Skudai, Malaysia
[b]Institute of Molecular Medicine and Biotechnology, Faculty of Medicine, Universiti Teknologi MARA Sungai Buloh Campus, Jalan Hospital, 47000 Sungai Buloh, Selangor, Malaysia
hasrinah@petroleum.utm.my

Membrane morphology plays an important role in achieving high flux and excellent uremic toxin removal for efficient hemodialysis therapy. Hemodialysis membrane morphology correlates to spinning parameters applied during fabrication of membrane. The effect of air gap on the morphology and liquid separation performance of the polysulfone (PSf) hemodialysis membrane is investigated. PSf hollow fibre membranes were prepared via dry-wet spinning process from dope solution comprises of 18 wt% PSf and 4.8 wt% polyvinylpyrrolidone in N-methyl-2-pyrrolidone. The membrane morphology was characterised using a scanning electron microscope (SEM) before tested with the ultrafiltration system to measure the pure water flux (PWF) and protein rejection using bovine serum albumin (BSA). SEM analysis revealed that the air gap does change the structure of the membranes due to the elongation stress because of the gravitational pull on the PSf hollow fibres. At low air gap (3 cm), the lower average pore size on the outer surface reduced the PWF while at high air gap (50 cm), the larger average pore size of membranes permitted water molecules to pass through easier and faster. It was observed that the PWF of the membrane increased significantly with air gap due to the increasing pore size. Membrane fabricated at 50 cm air gap obtained better PWF (28.45 $Lm^{-2}h^{-1}$) and protein rejection (94.47 %) compared to the membranes fabricated at 3 and 30 cm air gap. The effect of air gap enhanced the morphology and the performance of PSf membrane for hemodialysis application.

1. Introduction

In hemodialysis, the membranes used usually determine the success of the treatment. Hemodialysis removes excess moisture and metabolic waste (such as urea and creatinine) by diffusion and convection across the porous membrane and restores fluid and solute balance within the patient to some extent (Abidin et al., 2016). Polysulfone (PSf) is one of the promising polymeric materials that is widely used in separation field. PSf membranes show good heat resistance, physiochemical stability, resistance to chlorine, oxidation, and chemical compatibility over a wide range of pH (Yamashita and Sakurai, 2015). Although PSf membrane has been prevalently used, its hydrophobic character remains as the main disadvantage for liquid-liquid separation like hemodialysis. Many studies have concluded that the membrane fouling is related to hydrophobicity as reviewed by Khulbe et al. (2009). Modifying the pristine PSf has become the focus point before this to improve the hydrophilic character, which could enhance the biocompatibility of the PSf based-membrane. Polyvinylpyrrolidone (PVP), which is a hydrophilic polymer, is known to show good blood compatibility and has been commonly used in hemodialysis membrane formulation (Bowry et al., 2011).
In hemodialysis, the use of hollow fibre membrane is more preferable since it has a larger contact area with blood and the dialysate in spite of its small volume as a whole to exhibit excellent mass transfer efficiency (Feng et al., 2013). However, the preparation of the hollow fibre membrane is more complex than that of flat sheet because it involves more controlling parameter during the membrane spinning. The preparation of the hollow fibres often requires internal and external coagulants for the polymer to solidify and involves more

Please cite this article as: Said N., Hasbullah H., Ismail A.R., Abidin M.N.Z., Goh P.S., Othman M.H.D., Kadir S.H.S.A., Kamal F., Abdullah M.S., Ng B.C., 2017, The effect of air gap on the morphological properties of psf/pvp90 membrane for hemodialysis application, Chemical Engineering Transactions, 56, 1591-1596 DOI:10.3303/CET1756266

controlling parameters than those of flat sheet membranes such as the dimension of spinneret, dope viscosity, type of internal and external coagulants, flow rate of the bore fluid, type of bore fluid, dope extrusion rate, length and humidity of the air gap, wind-up speed, and fibre take-up speed (Korminouri et al., 2014).
Air gap has been reported before to play an important role in the development of membrane morphology with improved separation performance (Khayet, 2003). The fabrication of hollow fibre with a desirable morphology for a specific application is a tedious process and the effect of air gap on the hollow fibre membrane morphology and performance reported in the literature often provides contradict results especially in terms of the changes in morphology and separation performance. In fact, no study has ever discussed specifically the impact of applying different air gaps towards the membrane in the context of hemodialysis.
To resolve the confusion, this work attempts to do a quick study on the effects of air gap on the development of a desired PSf hemodialysis hollow fibre membrane. The main objective of this study is to understand the influence of air gap on the morphology of PSf/PVP90 hollow fibre membranes and figure out the membrane morphology that is needed to improve the membrane separation performance.

2. Experimental

2.1 Materials

All chemicals used were reagent grade. PSf (Udel-P1700) was purchased from Solvay Advanced Polymers; PVP-K90 (molecular weight = 360,000 g/mol) and bovine serum albumin (BSA) of > 98 % purity were obtained from Sigma Aldrich; NMP (98 %; molecular weight = 99.1 g/mol) was purchased from Merck.

2.2 Fabrication of PSf/PVP90 hollow fibre membranes

PSf polymer was dried in oven at 50 °C for 1 d to remove moisture content prior to dope solution preparation. Dope solution of 18 wt% PSf and 4.8 wt% PVP in NMP was prepared. The mixture was intensively stirred for one day to obtain a homogeneous solution. Before spinning, the dope was degassed for 6 h. The hollow fibre membranes were spun at room temperature by dry-wet spinning technique under different air gaps. The dope solution passed through a spinneret with an orifice diameter/inner diameter (OD/ID) of 0.6 / 0.3 mm, pressured using nitrogen gas, N_2 with the help of a gear pump to regulate dope extrusion rate (DER). The bore fluid, which is distilled water, was channelled into the spinneret using a constant-flow syringe pump. Coagulation bath used for phase inversion was tap water. The spinning parameters used were listed in Table 1. The fabricated membranes were treated in tap water for three days to remove the remaining solvent. The membranes were kept in 10 wt% glycerol to prevent the membrane structure from collapsing. After drying, the fibres were stored in sealed-plastic bags.

Table 1: Spinning parameters for hollow fibre spinning process

Air gap (cm)	3, 30, 50
Dope extrusion rate (mL/min)	1
Collection speed (m/min)	10
Bore fluid flow rate (mL/min)	1

2.3 Membrane characterisations

2.3.1 Scanning electron microscopy (SEM)

The structural morphology of PSf/PVP90 polymeric membrane was examined using SEM. The polymeric membrane was snapped in liquid nitrogen to obtain clear and smooth cross-section, before sticking onto metal plate using double-sided carbon tape at lateral sides. For surface studies, a small piece of each membrane was mounted on the metal plate horizontally. The membrane sample was sputter-coated with platinum/palladium mixture before being analysed. The images of outer surface and cross-section of the membrane were collected.

2.3.2. Porosity and pore size measurement

Dry-wet weight method was used to measure membrane porosity, ε. The membrane was immersed in pure water for 1 h. Next, the membrane weight was measured in both wet and dry condition. The porosity of the membrane was defined in the following Eq(1):

$$\varepsilon = \frac{w_1 - w_2}{V\rho w} \quad (1)$$

where ε is the porosity of the membrane (%), w_1 is the mass of the wet membrane, w_2 is the mass of the dry membrane, V is the volume of the membrane and ρw is the density of water (1.0 g/cm^3). The average pore

radius, r (m) was determined by the filtration velocity method (Abidin et al., 2016), using Guerout-Elford-Ferry Eq(2):

$$r = \sqrt{\frac{(2.9 - 1.75\,\varepsilon) \times 8\eta l Q}{\varepsilon \times A \times \Delta P}} \quad (2)$$

where η is the water viscosity at 25 °C, l is the membrane thickness (m), Q is the volume of the permeate water per unit time (m^3/s), A is the effective area of membrane (m^2) and ΔP is the operational pressure (Pa). Pore size (diameter) of membrane was determined by multiplying r by 2.

2.4 Evaluation of membrane separation performance

The PWF, J and BSA rejection, R of the membranes were measured to evaluate the membranes separation performance. Membrane modules consist of 10 fibres (10 cm in length) were potted using epoxy. The PWF was obtained at the trans-membrane pressure of 0.74 bar using the following Eq(3):

$$J = \frac{V}{A \times \Delta t} \quad (3)$$

where J represents the PWF ($L\ m^{-2}\ h^{-1}$), V is the volume of permeate (L), A is the effective surface area (m^2) and Δt is the permeation time (h). For protein rejection test, 500 ppm BSA solution was used. The percent rejection was calculated by Eq(4).

$$R\,(\%) = \left(1 - \frac{Cp}{Cf}\right) \times 100\,\% \quad (4)$$

where C_p and C_f are the BSA concentrations of the permeate and feed. The concentration of BSA was measured using UV-Vis Spectrophotometer (DR 5,000).

3. Results and discussion

3.1 Morphologies of PSf/PVP90 membranes

Based on Table 2, both inner and outer diameters of the membrane decreased with the increasing air gap. This was due to the elongation stress created on the fibre by gravitational pull. The stress may affect the molecular orientation during membrane formation which leads to significant changes in membrane characteristics. The subsequent effect of elongation stress on the membrane properties is further discussed in Section 3.2.

Figure 1 represents the SEM micrographs taken from the cross section and the outer surface of the PSf/PVP90 hollow fibre membranes fabricated at the different air gaps. Membranes spun at 30 cm and 50 cm air gap have led to the formation of one long array of finger-like structure, which originated from the inner side of membrane. The finger-like void for membrane spun at 50 cm air gap was longer and bigger compared to the membrane fabricated at 30 cm air gap. This was due to the greater elongation force exerted at higher air gap which reduced the thickness of polymer solution, allowing faster solvent-non solvent exchange at the inner side of fibre (Khayet, 2003). The formation of porous sponge-like structure at the outermost layer of the membrane was due to the exchange of solvent and air moistures during residence time. The dense selective skin layer at the innermost region of the membrane was formed by instantaneous de-mixing between solvent and non-solvent (Abdelrasoul et al., 2015). The results are in accordance with the desired properties of hemodialysis membrane, in which the inner surface possessed the smallest pores to prevent clogging of solutes inside the pores (Yamashita and Sakurai, 2015). The nano-sized pores at the selective layer are able to minimise the transport of human albumin while permitting other smaller toxin molecules to pass through.

Table 2: Dimensional changes of hollow fibre membranes as a function of air gap

Air gap (cm)	Residence time (s)	OD (cm)	ID (cm)	OD/ID Ratio	Cross-Section Area Change Ratio[a]
3	0.38	0.045	0.036	1.25	3.70
30	3.82	0.035	0.023	1.52	3.80
50	6.36	0.031	0.020	1.55	4.81

[a]Ratio of the spinneret cross-section area to a fibre cross-section area.

The membrane fabricated at 3 cm air gap produced a sandwich-like structure which consists of two selective skin layers and two arrays of finger-like voids. At very low air gap, the exchange of solvent and moistures at

the membrane outer surface cannot take place due to very short residence time. As the flow of bore fluid solidifies the membrane inner surface instantaneously, the same thing has happened at the outer surface of the nascent hollow fibre membrane as the membrane entered straight away into the coagulation bath. The identical dense skin layer to the inner surface was formed at the outer layer of the membrane. This kind of morphology is not recommended for hemodialysis application since it could promote the entrapment of protein molecules inside the membrane matrix.

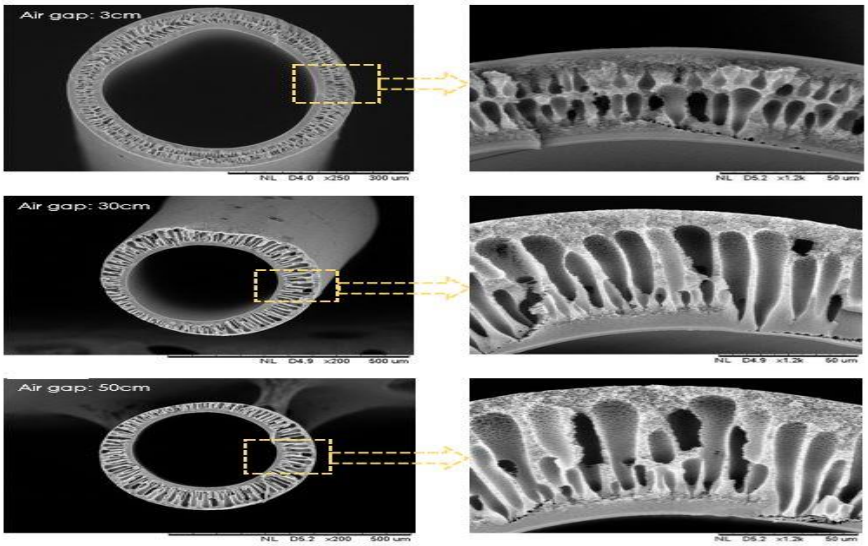

Figure 1: The cross-sectional SEM images of membrane fabricated at air gap of 3 cm, 30 cm, and 50 cm

From Figure 2, the pore size at the membrane outer surface became larger as the air gap is increased. The increasing air gap enhanced the formation of larger pores at outer surface. Moisture induced phase inversion which occurred at high air gap created pores at the outer side of membrane before the membrane enters the coagulation bath. The longer the membrane takes to reach the coagulation bath, the larger the pore size. Polymer nucleation was allowed to happen longer at high air gap. In hemodialysis application, the larger membrane pore size at the outer surface promotes the removal of bigger uremic toxins through convection.

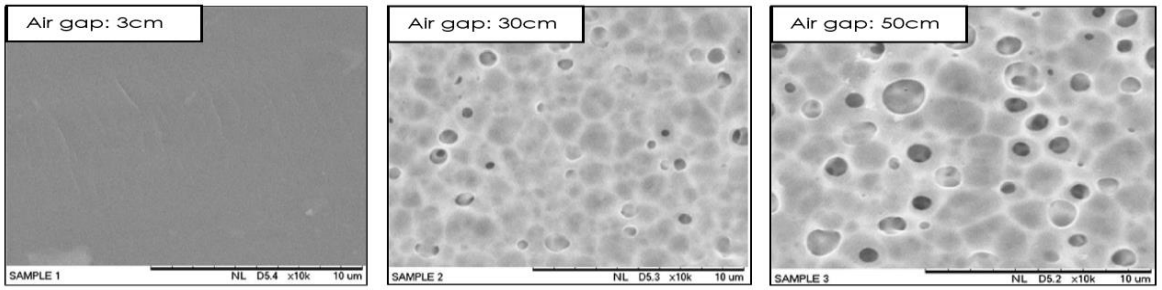

Figure 2: The SEM images of PSf/PVP90 membrane outer surface fabricated at air gap of 3 cm, 30 cm, and 50 cm

3.2 Average pore size and porosity of PSf/PVP90 membranes

Table 3 shows the results of average pore size and porosity of the membrane fabricated at different air gaps. The average pore size of PSf/PVP90 hollow fiber membrane was calculated based on water permeation data. The membrane experienced a substantial increment of average pore size with the increase of air gap. The porosity also increased with increasing air gap due to the changes in membrane morphology as shown in Figure 1 and 2. Higher air gap means that the membrane has been exposed longer to gravitational pull, causing the huge effect towards membrane structure and eventually produces a bigger pore size compared to membrane fabricated at lower air gap. Macromolecules inside the solution experienced swelling and relaxation once the solution is extruded from spinneret, changing the orientation of macromolecules inside the

membrane. This later produced a larger membrane average pore size which could permit water to pass through easier and faster.

In terms of porosity, membrane spun at 50 cm and 30 cm air gap were by far more porous as shown in Table 3. The sufficiently strong elongation stress during spinning has pulled the polymer molecular chains apart at the beginning of phase separation and created porous structure. This resulted in the increase of the membrane free volume (Cao et al., 2004). The formation of longer and bigger finger-like structures as the result of faster phase inversion also helped to accommodate pure water. On the other hand, the weak stress exerted on the membrane spun at 3 cm air gap had induced the unfavourable change in molecular orientation which reduced membrane porosity or free volume (Khayet, 2003).

Table 3: Results of porosity and average pore size

Air gap (cm)	Porosity (%)	Average pore size (μm)
3	17.13	0.018
30	44.13	0.039
50	46.67	0.044

3.3 The effect of air gap on membrane separation performance

A more porous membrane structure is able to facilitate water movement across the membrane. As stated by previous study (Santoro and Guadagni, 2010), a high flux membrane can achieve a better removal of middle molecular uremic toxins by the mean of convection.

The results of PWF and BSA rejection with respect to various air gaps are shown in Figure 3. Significant improvement in PWF was reported as the air gap is increased. The longer and larger finger-like voids helped in facilitating pure water more efficient. The PWF of membrane spun at 3 cm air gap was very low due to its dual-skin layer property and small average pore size.

As for the protein rejection, all the membranes obtained more than 90 % rejection of BSA which was quite compulsory for all hemodialysis membranes to prevent albumin loss. Too much albumin loss could render albumin loss syndrome to the dialysis patient (Irfan et al., 2014). The main reason would be the compact arrangement of nano-sized pores at the membrane skin layer, which restrained the movement of BSA molecules across the membrane. The results (Figure 3) proved that BSA rejection can be influenced by different membrane morphologies. The trend shows the enhanced BSA rejection as the PWF increases. This happened due to the improved route for water molecules to pass through, leaving the large and hydrophobic BSA molecules behind. As the pure water moving faster, the hydrophobic nature of BSA with the help of the membrane selective layer had weakened the interaction between the protein molecules and water molecules.

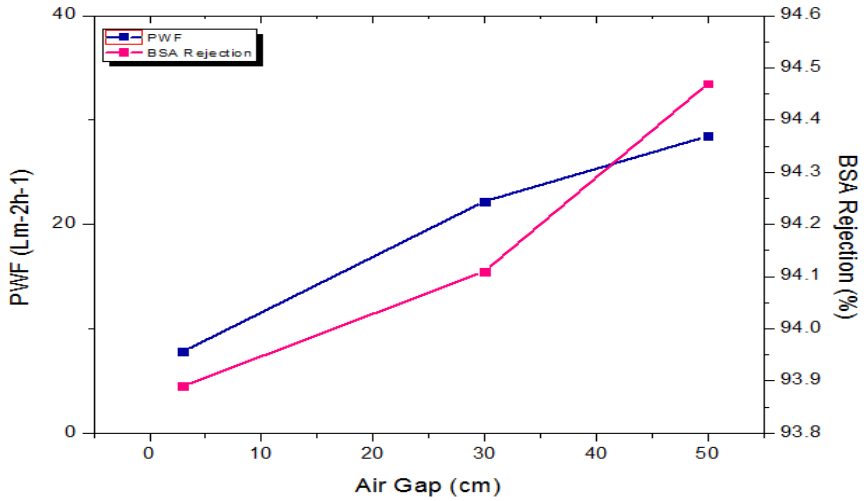

Figure 3: PWF and BSA rejection of the membranes

4. Conclusion

In this work, air gap has been manipulated during the fabrication of PSf/PVP90 hollow fibre membranes. The membrane spun at low air gap (3 cm) showed a sandwich-like structure while membranes spun at higher air

gap (30 cm and 50 cm) possessed an asymmetrical structure with skin layer, compact spongy sublayer and finger-like structure with macro-voids. The porosity and pore size of the membrane increased with the increase in air gap. The same trend could be seen on the PWF of the membrane while maintaining excellent protein resistance. All the results indicated that air gap is one of the spinning parameters that should be focused on during hollow fibre membrane fabrication process to acquire the desired membrane morphology for hemodialysis application.

Acknowledgements

We gratefully acknowledge the financial support from the Universiti Teknologi Malaysia and Ministry of Higher Education Malaysia (Grant no: 01G46 and 4F652).

References

Abdelrasoul A., Doan H., Lohi A., Cheng C.H., 2015, Morphology control of polysulfone membranes in filtration processes: a critical review, Chemical and Biomolecular Engineering Review 2, 22–43.

Abidin M.N.Z., Goh P.S., Ismail A.F., Othman M.H.D., Hasbullah H., Said N., Kadir S.H.S.A., Kamal F., Abdullah M.S., Ng B.C., 2016, Antifouling polyethersulfone haemodialysis membranes incorporated with poly (citric acid) polymerized multi-walled carbon nanotubes, Materials Science and Engineering: C 68, 540–550.

Bowry S.K., Gatti E., Vienken J., 2011, Contribution of polysulfone membranes to the success of convective dialysis therapies, Eds. Saito A., Kawanishi H., Yamashita A.C., Mineshima M., High performance Membrane Dialyzers, 1st Ed., Karger Publishers, Basel, Switzerland, 110–118.

Cao C., Chung T.S., Chen S.B., Dong Z.J, 2004, The study of elongation and shear rates in spinning process and its effect on gas separation performance of Poly(ether sulfone) (PES) hollow fiber membranes, Chemical Engineering Science 59 (5), 1053-1062.

Feng C.Y., Khulbe K.C., Matsuura T., Ismail A.F., 2013, Recent progresses in polymeric hollow fiber membrane preparation, characterization and applications, Separation and Purification Technology 111, 43–71.

Irfan M., Idris A., Yusof N.M., Khairuddin N.F.M., Akhmal H., 2014, Surface modification and performance enhancement of nano-hybrid f-MWCNT/PVP90/PES haemodialysis membranes, Journal of Membrane Science 467, 73–84.

Khayet M., 2003, The effects of air gap length on the internal and external morphology of hollow fiber membranes, Chemical Engineering Science 58, 3091–3104.

Khulbe K.C., Feng C., Matsuura T., 2009, The art of surface modification of synthetic polymeric membranes, Journal of Applied Polymer Science 115, 855–895.

Korminouri F., Rahbari-Sisakht M., Rana D., Matsuura T., Ismail A.F., 2014, Study on the effect of air gap length on properties and performance of surface modified PVDF hollow fiber membrane contactor for carbon dioxide absorption, Separation and Purification Technology 132, 601–609.

Santoro A., Guadagni G., 2010, Dialysis membrane: From convection to adsorption, NDT Plus 3, 36–39.

Yamashita A.C., Sakurai K., 2015, Dialysis Membranes-physicochemical structures and features, Ed. Suzuki H., Updates in Hemodialysis, 1st Ed., Intech, Rijeka, Croatia, 159–187.